Energy dissipation downstream of dams established in alluvial beds

A. Sá Lopes, M.F. Proença & R. Maia
Departamento de Engenharia Civil, Faculdade de Engenharia da Universidade do Porto, Rua Dr. Roberto Frias, 4200-465 Porto, Portugal

ABSTRACT: Energy dissipation behind the hydraulic structure of a mobile dam was experimentally studied with the aid of Laser-Doppler Anemometry (LDA), aiming to optimize the design and length of the dissipation devices, most commonly a stilling basin followed by rock fill alluvial bed protection.
Measurements of the flow field over the rock protection were carried out in order to prevent damages at the foundations of the structure as well as to protect the river bed from erosion, namely due to operational reasons. The characterisation of mean velocity and turbulence intensities were carried out for different flow conditions and different rock fill characteristic dimensions, using a physical model of the Crestuma dam, located in the Douro river.
The obtained results (namely values of bottom shear stress) provide a better insight of the rock fill protection behaviour and can help to achieve a cheaper and safer design of the rock fill protection.

1. INTRODUCTION

Energy dissipation of flood discharges is a very important issue that must be carefully analysed when bearing in mind the design and layout of hydraulic structures, namely dams. The usual formation of a hydraulic jump downstream the weir devices requires adequate protection of the river bed, at locations where energy dissipation occurs and where flow velocities present higher values, especially if the constructions are established in alluvial beds.

Stilling basins concrete slabs followed by rock fill bed protections are one of the most common devices that are used to allow weir discharges to be performed without damaging the construction foundation. Length and characteristics of the protected zone and, specially, the rock fill bed protection depend on flow conditions and have to be carefully defined in order to prevent erosion or scour of the river bed.

Flow velocity and bed shear stress values play an important role in the process and have been the basis for the establishment of different criteria, allowing initiation of movement prediction.

In the present work an experimental study of a physical model of the Crestuma dam was carried out. Flow field definition for different flow conditions and different bed rock protections were made using laser Doppler anemometry technique in order to allow the analysis of velocity flow characteristics in each situation. Rock fill protection behaviour, concerning scour and erosion occurrence, has been studied in relation to flow field type changes.

Bottom shear stress values have been calculated and compared with the literature (Shields diagram) in order to try to explain any possible erosion effects. Two different approaches to Shields diagram have been made, taking into account the existence or not of flow uniformity characteristics of the studied flow. In accordance, two different methods of evaluation of friction velocity values have been applied.

2. THEORETICAL FRAMEWORK

In 1936, Shields described the initial bed grain instability problem based on experimental data. Shields diagram was referred to plane beds with grains of uniform size and was modified in order to take into account the non uniform distribution of the mixtures of different grains and their orientation under flow conditions. The modified Shields diagram (Fig. 1) presents several curves instead of the original one, grading different levels

of incipient motion of the particles as referred by Hoffmans et al. (1997).

For a particular situation the critical shear stress value can be obtained through the Shields parameters ψ and D_* definition, assuming:

$$\Psi = \frac{u_*^2}{\Delta g d} \quad and \quad D_* = d\left(\frac{\Delta g}{\nu^2}\right)^{\frac{1}{3}} \tag{1}$$

where : Δ = relative density ((ρ_s/ρ) -1); d = particle diameter ($d = d_{50}$); u_* = friction velocity; g = acceleration of gravity; ν = cinematic viscosity; ψ, mobility parameter; D_*, dimensionless diameter.

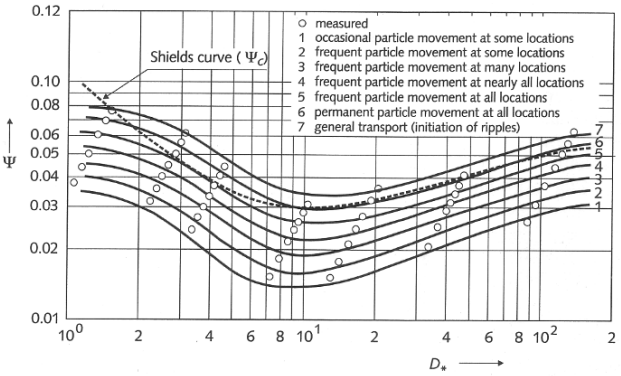

Figure 1. Modified Shields Diagram (Hoffmans et al. 1997).

Shields diagram application requires the knowledge of flow and bed sediment characteristics.

Flow uniformity can be checked plotting u/U_{max} versus y'/h on different sections and verifying if the velocity profiles overlap on a single curve with the following law:

$$\frac{u(y')}{U_{\max}} = A\ln\left(\frac{y'}{h}\right) + B \tag{2}$$

where u = mean flow velocity; y' = vertical distance to the bed flow, corrected according to rough bed situation; U_{max} = maximum velocity profile; h = flow depth; and, A and B constants.

The above equation will not be valid if the following conditions are not fulfilled (Rota criterion 1962, according to Cardoso 1990):

$$\left.\begin{aligned} &\frac{u_*}{U_{\max}} = constant \\ &\beta = \frac{\rho h g\left(-I_0 + \frac{\delta h}{\delta x}\right)}{\tau_0} = constant \\ &\frac{d\left(\frac{U_{\max}\delta_*}{u_*}\right)}{dx} = constant \end{aligned}\right\} \tag{3}$$

where I_0 is the bottom slope, δ_* and τ_0, are the boundary layer momentum thickness and the shear stress values, respectively. For β values: < -1, accelerated flow; = -1, uniform flow; > -1, decelerated flow.

Non-uniformity may then concern a set of flows which equilibrium is affected by the upstream flow conditions. Corresponding velocity profiles will vary along the flow.

Friction flow velocity evaluation must be done taking into account the referred flow characteristics.

For uniform flow, the general equation, most commonly used is:

$$u_* = (gRJ)^{\frac{1}{2}} \tag{4}$$

where R is the hydraulic radius and J the energy loss by unit length, that can be given by the Manning-Strickler expression:

$$J = \frac{U^2}{K_s^2 R^{\frac{4}{3}}} \tag{5}$$

where K_s (=l/n) is the Strickler coefficient and U the mean sectional velocity. For uniform flows with small bottom gradient, R may be usually taken as h, the flow depth, and J as I_o, the bottom channel slope.

Regarding non-uniform flows using Saint Venant equations and according to Graf & Song (1995) and Graf & Altinakar (1998) the friction velocity can be given by:

$$u_*^2 = ghI_0 + \left(-gh\frac{\delta h}{\delta x}(1 - Fr^2)\right) \tag{6}$$

where I_0 is the bottom channel slope, x the velocity profile coordinate and Fr the Froude number, which is defined as:

$$Fr = \frac{U}{\sqrt{gh}}$$

3. EXPERIMENTAL SET UP

3.1 Facilities and measuring equipment

Experiments have been carried out in a water channel of the Hydraulics Laboratory of FEUP. The water channel, with a length of 32,3m, a width of 1,0m and a bottom slope of 0,5%, is provided with side windows allowing visual access to the test sections.

The channel is fed from a reservoir located at a higher level, provided with a water level control allowing a constant flow to be delivered to the channel.

Flow measurement values can be controlled, upstream through a flow meter, Sparling Waterhawk series 600, flangeless version, and downstream through a sluice crested weir whose

discharge value is obtained measuring the water level by means of a Bestobell Mobrey MSP90 system.

Velocity measurements have been made using a one component fibre optics Laser System from Dantec, working in forward scatter mode.

A 100 MW Argon-Ion laser source, operating in multi-mode was used.

The main characteristics of the Laser Doppler Anemometer system are shown in table 1.

Table 1. Laser Doppler anemometer characteristics.

Laser wave length	514,5 nm
Half angle of measuring beams in air	3,65º
Shift frequency	0,6 MW
Beam expansion ratio	1,95
Dimensions of control volume in air:	
Major axis	2,53 mm
Minor axis	1,62 mm
Fringe Spacing	4,04 mm
Frequency Shift	0,6 Mw

The signal from the photomultiplier was band-pass filtered and processed by a TSI 1990c counter, operating in the single measurement per burst mode, with a frequency validation of 1% at 10/16 cycle comparison. A 1400 Dosteck card interfaced the counter with a computer, which provided all statistical quantities, using a purpose's built software.

3.2 Physical model characteristics and similarity conditions

In order to perform experimental work a physical model of Douro river Crestuma dam was built.

Crestuma dam is a mobile type dam founded on alluvial bed, whose flow discharges are made through double slicing gates installed on 8 spans of 28 m each and supported by 49 m length and 6 m width piles. The double slicing gates can move independently and allow discharges over or underneath their body or both simultaneously. Flow discharge energy dissipation is achieved on a concrete slab stilling basin with a length of 42 m from gate axis position, followed by the rock fill bed protection with a length of 80 m.

The model was made of perspex using a 1:80 geometric scale. Taking into account that gravitational forces are predominant in this case, the Froude number similarity was used for model construction.

Considering the above mentioned scale and taking into account the width of the water channel of Hydraulics Laboratory (1m), the portion of Crestuma dam represented by the model includes one central span, two piles and two lateral incomplete spans (approximately half spans) as represented in Figure 2.

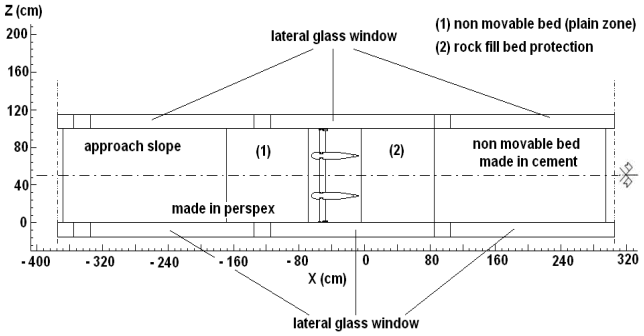

Figure 2. Crestuma model – plant.

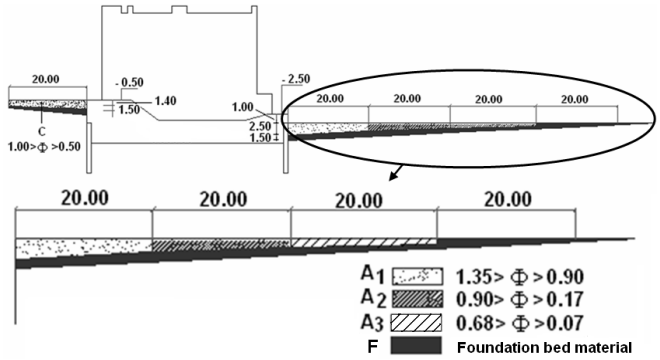

Figure 3. Crestuma dam rock fill bed protection characteristics.

Crestuma rock fill protection has a variable depth and includes different number of layers along its length as shown on Figure 3, where rock fill material dimensions are also indicated.

The concrete slab basin of the plant was modelled on Perspex and the rock fill protection by means of granite and sand grains with specific weights of:

- Granite grains – 26 KN/m^3
- Sand grains – 16 KN/m^3
- Wet sand grains – 18 KN/m^3

The four top layer sections used in the model were 25 cm length each and will be referred as section 1, 2, 3 and 4, corresponding to the above A1, A2, A3 and F designations. Section 4 corresponds to natural foundation bed material.

The bed grain size distribution used for the different sets of experiments corresponds to three different rock fill protection characteristics, A, B and C, as shown on table 2. The rock fill bed protection designated as type A corresponds to the scaled rock fill bed protection used in Crestuma dam. Type B section (increased) dimension was designed taking into account market maximum available dimensions of rock fill to be used in section 1 of the prototype. Type C section 1 element dimensions (the largest of all three) were determined using the following formula proposed

by U.S. Corps of Engineers, and used on Crestuma project (LNEC, 1972):

$$d \geq k \frac{U^2}{2g} \frac{\gamma}{\gamma_s - \gamma}$$

where γ and γ_s are respectively the specific weights of water and rock material, k is dependent on flow turbulence and was taken equal to 1,35.

Sections 2 and 3 element dimensions of types B and C rock protections have been evaluated regarding to grading correspondence to section 1 elements dimension used on type A (Crestuma Project) rock fill protection.

Table 2. Model rock fill bed protection characteristics.

		Rock fill bed protection		
		Type A (cm)	Type B (cm)	Type C (cm)
Section 1	d_{35}	1,32	1,85	2,85
	d_{50}	1,50	2,00	3,00
	d_{65}	1,55	2,15	3,15
	d_{75}	1,60	2,25	3,25
	d_{84}	1,76	2,34	3,34
	d_{85}	1,77	2,35	3,35
	d_{90}	1,81	2,40	3,40
Section 2	d_{35}	0,72	0,85	1,19
	d_{50}	0,80	1,00	1,35
	d_{65}	0,82	1,15	1,52
	d_{75}	0,90	1,25	1,63
	d_{84}	1,36	1,34	1,72
	d_{85}	1,37	1,35	1,74
	d_{90}	1,41	1,40	1,80
Section 3	d_{35}	0,66	0,71	0,95
	d_{50}	0,70	0,75	1,05
	d_{65}	0,75	0,80	1,16
	d_{75}	0,80	0,83	1,22
	d_{84}	1,12	0,85	1,23
	d_{85}	1,17	0,86	1,30
	d_{90}	1,20	0,87	1,33

3.3 Flow Conditions

As previously mentioned Crestuma gates allow different types of discharges. In the present work flow discharge was considered to be done always by the sections underneath the gates and keeping equal gate openings in all the three spans of the model.

Two different flow values have been considered, 11,5 l/s and 12,2 l/s, which main features are presented on table 3, where H_1 is the upstream water level and y_0 is the downstream water level.

Table 3. Main flow characteristics.

Flow value (l/s)	11,5	12,2
H_1 (mm)	165	165
y_0 (mm)	58,5	60,5
Froude nb	5,81	5,79
Gate opening (mm)	9	12,5

The 11,5 l/s value corresponds to a flow situation where hydraulic jump is formed within the stilling basin slab. A small increase of 6 % to 12,2 l/s, on the flow value, led to an hydraulic jump showing much more instable characteristics with an oscillatory behaviour and a tendency to move away from the stilling basin slab.

4. EXPERIMENTAL RESULTS

Taking into consideration the two referred flow conditions and the three different types of rock fill bed protection, four sets of measurements have been carried out.

On each of them, mean and fluctuating velocity profiles have been measured at different flow sections behind the hydraulic structure, as shown on Figure 4.

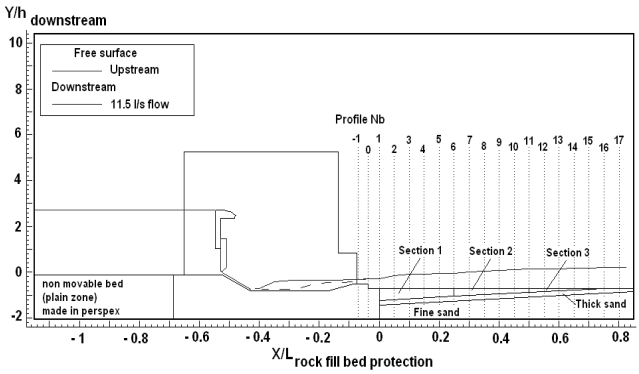

Figure 4. Location of measured profiles.

The first set of experiments concerned a gate flow discharge value of 11,5 l/s and the use of a rock fill bed protection, designated as type A.

Mean and fluctuating values of the horizontal and of the vertical velocity components for the different profiles above referred have been measured and led to the results shown on Figures 5a) and 5b). Values of velocities and depth presented are dimensionless taking as reference respectively the horizontal mean sectional velocity and the flow depth values of the stabilized flow on the sections downstream the rock fill bed protection.

As already stated the flow characteristics showed a quite stable hydraulic jump formed within the stilling basin slab. The highest velocity values were observed before entering the rock fill bed protection and no erosion was verified.

The second set of measurements concerned the same type A of rock fill bed protection but a higher gate flow discharge value of 12,2 l/s. Flow characteristics showed a quite unstable and

oscillating hydraulic jump moving periodically away from the stilling basin slab.

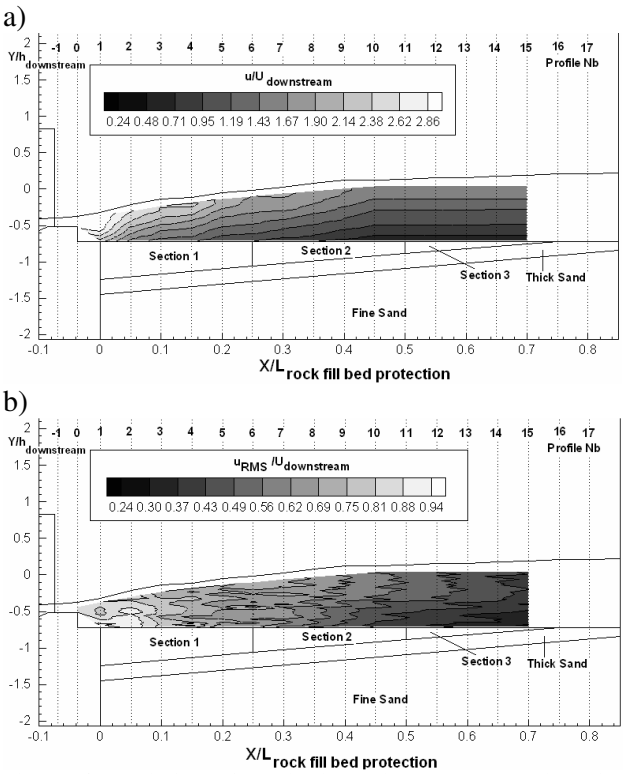

Figure 5. Evolution of the horizontal component values for 11,5 l/s flow and type A rock fill protection: a) mean velocity and b) rms (note: dark values are the lowest in range).

The consequence of this type of flow gate discharge was the start of the formation of a scour hole on the rock fill bed protection, whose characteristics, concerning dimensions and location, are shown on Figure 6. Scour hole depth values were made dimensionless by considering the ratio to the downstream flow depth value. The scour hole was mostly located in front of the central gate span, along section 1 of the rock fill bed protection. Stabilization of sediment transport occurred, approximately, two hours after the starting of the test.

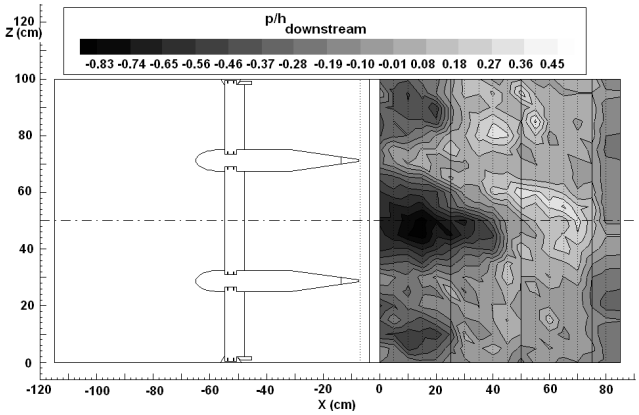

Figure 6. Scour hole caused by a 12,2 l/s gate discharge on type A rock fill bed protection.

Mean and fluctuating horizontal velocity component values, after sediment transport stabilization, are presented on Figures 7a) and 7b).

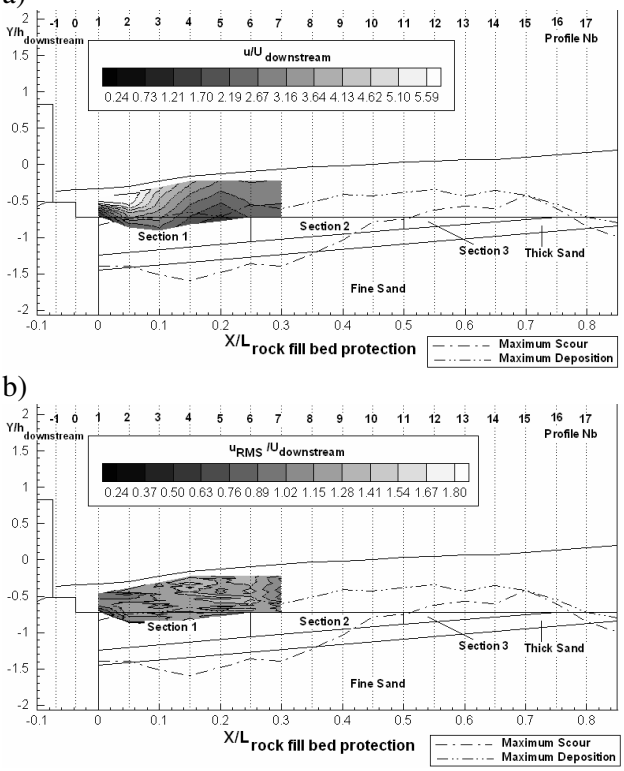

Figure 7. Evolution of the horizontal component values for 12,2 l/s flow and type A rock fill protection: a) mean velocity and b) rms (note: dark values are the lowest in range).

Figures 7a) and b) also represent longitudinal profiles of maximum scour and of maximum deposition, the first corresponding to the central channel axis and the other to the pile axis, in accordance with eroded material being transported and deposited downstream, at different transverse rates and locations. The deposition of that material turned the velocity measurement on some downstream profiles impossible because measuring points were out of reach of laser beams. Moreover, only horizontal velocity component could be measured due to the very low flow depth associated with very high flow surface fluctuations and because of LDA system characteristics, namely beam separation at front lens probe.

A comparison of velocity flow fields of 11,5 l/s and 12,2 l/s flows is presented on Figure 8 a) and b).

These figures enable to conclude that much higher velocity values and much more important velocity gradient values on the rock fill protection region have been achieved with the 12,2 l/s flow, due not only to the flow velocity values increase,

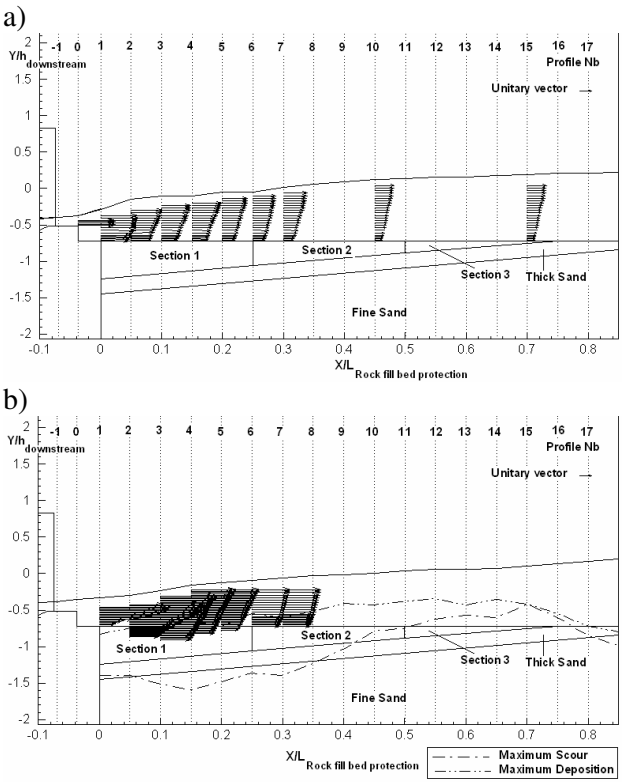

Figure 8. Flow fields for a) 11,5 l/s and b) 12,2 l/s gate flow discharges and for type A rock fill bed protection.

but as well as to the tendency of movement of the hydraulic jump towards downstream.

The third set of experimental measurements was carried out with the same flow gate discharge of 12,2 l/s but using type B rock fill protection.

Scour process did not start immediately. Several oscillations could be noticed on the material of upstream measuring sections (1 and 2) of top layer rock protection during the first 24 h of the test, which have been followed by the formation of the scour hole presented on Figure 9.

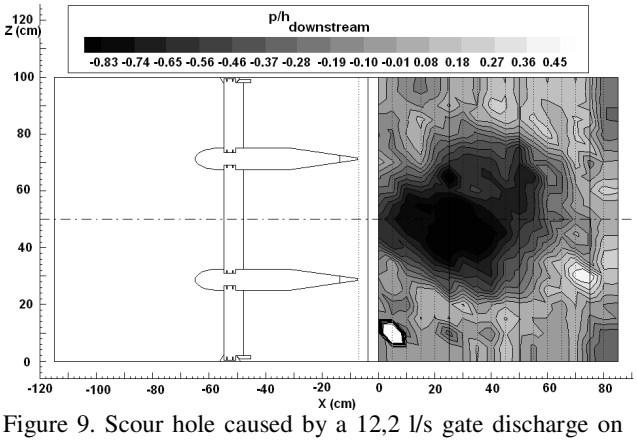

Figure 9. Scour hole caused by a 12,2 l/s gate discharge on type B rock fill protection.

The scour hole position moved downstream, in comparison with the situation previously reported for type A rock fill (Fig. 6), and it was now located at the end of section 1 and beginning of section 2 of the rock fill bed protection.

Mean and fluctuating horizontal component velocity measurements have been made before and after the scour hole formation and the results are presented on Figures 10 a) and b).

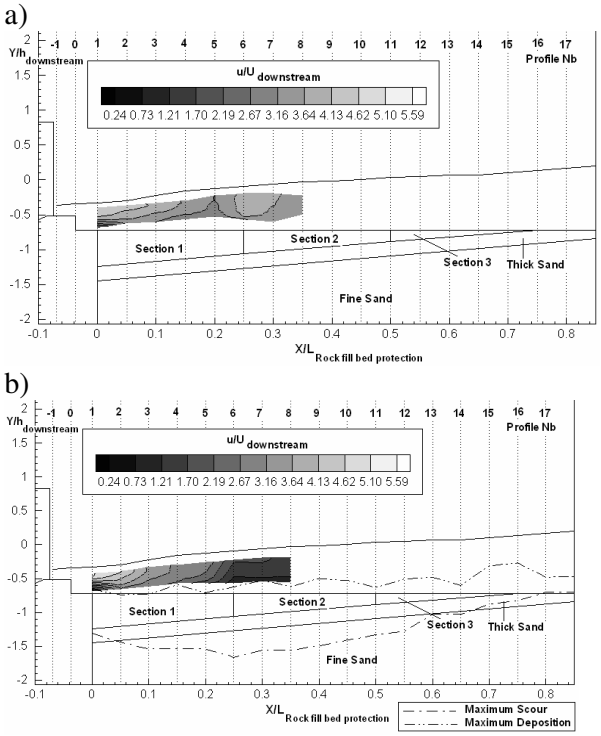

Figure 10. Evolution of horizontal component mean velocity values for 12,2 l/s flow and type B rock fill protection: a) before and b) after scour hole formation (note: dark values are the lowest in range).

As shown on these figures, the two experiments do show similar mean horizontal component velocity profiles at the beginning of the rock fill protection. Higher differences can be noticed on velocity profiles P5 to P8, corresponding to the end of section 1 and beginning of section 2 of the top rock fill layer protection. The analysis of Figures 11a) and 11b), concerning corresponding horizontal component fluctuating velocity values, shows that after scour hole formation the highest fluctuation values have moved towards section 1 zone of bed protection whilst, before erosion was noticed, those values were located by the end of section 1 and beginning of section 2.

The last set of measurements concerned the rock fill bed protection type C and again the use of the same gate flow value of 12,2 l/s.

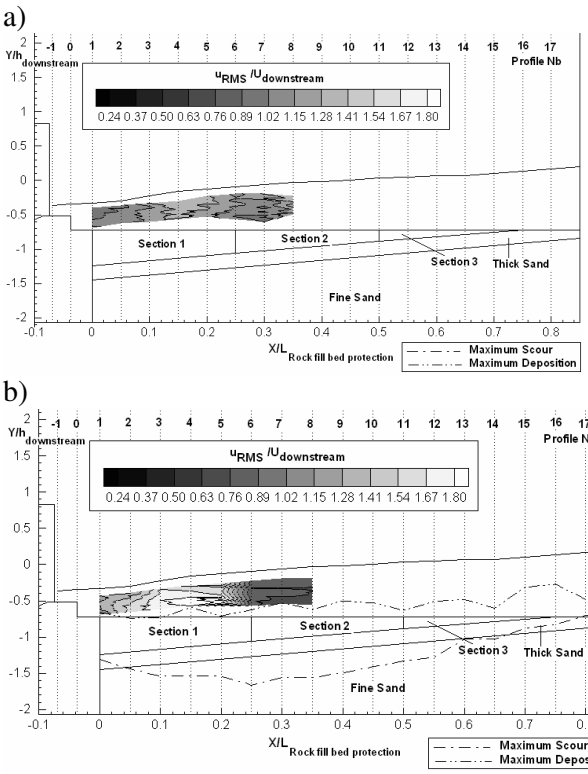

Figure 11. Evolution of horizontal component rms values for 12,2 l/s flow and type B rock fill protection: a) before and b) after scour hole formation (note: dark values are the lowest in range).

During the corresponding tests no erosion was noticed on sections 1 and 2 of the rock fill protection. Only slight erosion of the material of section 3 could be observed. Related scour hole characteristics are presented in Figure 12.

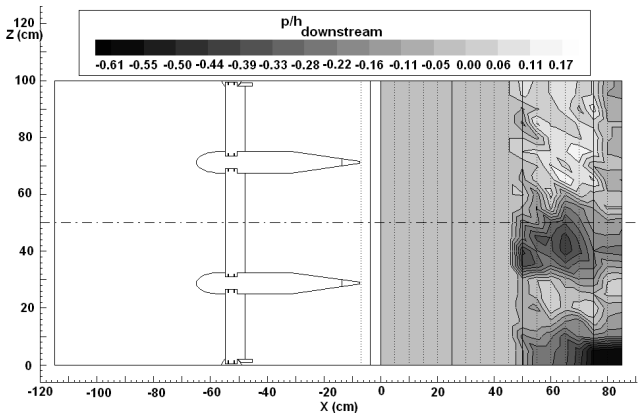

Figure 12. Scour hole caused by a 12,2 l/s gate discharge on type C rock fill bed protection.

Horizontal component mean and fluctuating velocity values are presented on Figures 13a) and 13b).

It can be confirmed that mean velocity values are quite similar to the 11,5 l/s flow case. In what concerns fluctuating values, less instability was noticed in this case.

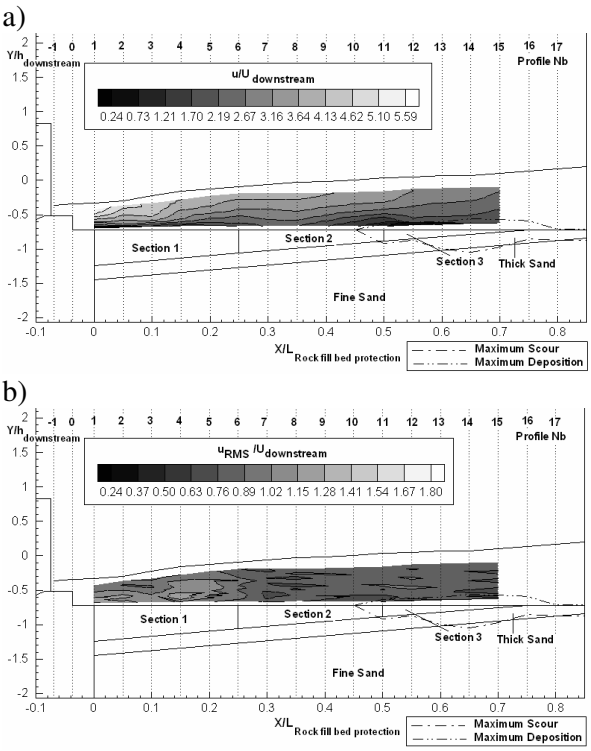

Figure 13. Evolution of horizontal component values for 12,2 l/s flow and type C rock fill protection: a) mean velocity and b) rms (note: dark values are the lowest in range).

A comparison of the mean flow velocity fields for 12,2 l/s flow regarding rock fill types B (after sour occurrence) and C is made on Figures 14a) and b).

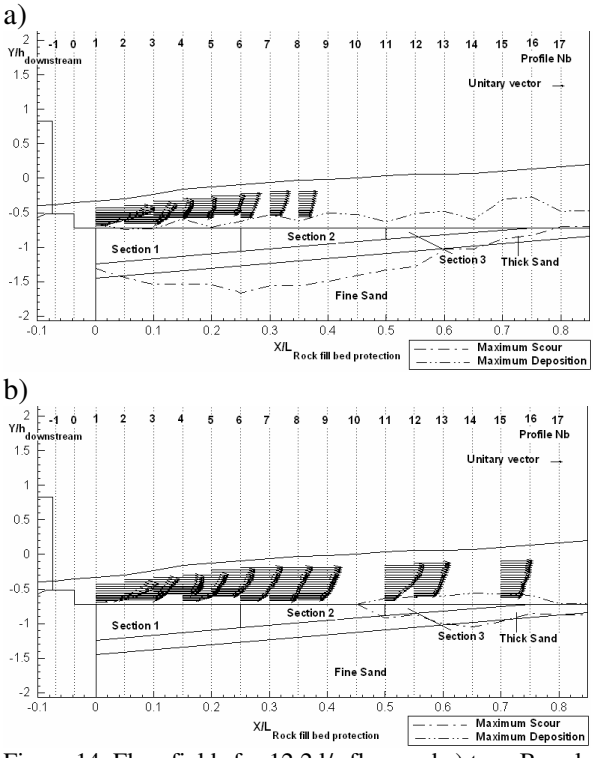

Figure 14. Flow fields for 12,2 l/s flow and a) type B rock fill protection (after scour occurrence) and b) type C rock fill protection.

This information complements Figure 8b), enabling to compare influence of rock fill protection dimension.

5. RESULT ANALYSIS

The results, earlier presented have been analysed bearing in mind the rock fill bed protection behaviour, concerning its characteristics and flow conditions.

Result analysis has been carried out considering Shields criterion for initiation of movement of gravel particles on a flat bed, using the modified Shields diagram, presented on Figure 1.

The application of Shields diagram and the mobility values calculation required the definition of the friction velocity values. That has been made considering the flows under study either as uniform or as non-uniform flows.

For uniform flows, friction velocity values, u_*, have been directly assessed by using the expressions (4) and (5), and assuming Strickler coefficient as previously referred:

$$K_s = \frac{1}{n}$$

where, according to Chang (1988), n is given by:

$$n = 0{,}0482(d_{50})^{\frac{1}{6}}$$

That allowed bed shear stresses (τ_o) and Shield's parameters (D* and ψ) to be evaluated (based on equation 1) for flow profiles not affected by scour hole formation. Table 4 exemplifies the evaluation of u_* for 12,2 l/s flow, type C rock fill protection. For this same flow and types A and B rock fill bed protection, this method enabled only to evaluate those parameters for the entrance of the rock fill protection area (profile P1). Figure 15 (a, b and c) shows plots of the correspondent obtained values.

Table 4. Friction velocity values evaluation for 12,2 l/s flow value and type C rock fill protection (uniform flow)

Profile	x	h	R	U	J	u_*
	cm	cm	cm	m/s	m/m	cm/s
P1	0	2,4	2,3	0,821	7,49E-02	12,97
P2	5	2,6	2,5	0,758	5,77E-02	11,83
P3	10	3,0	2,8	0,729	4,44E-02	11,11
P4	15	3,4	3,2	0,652	3,04E-02	9,74
P5	20	3,6	3,4	0,599	2,39E-02	8,87
P6	25	3,8	3,5	0,592	1,67E-02	7,62
P7	30	4,0	3,7	0,623	1,74E-02	7,95
P8	35	4,2	3,9	0,630	1,67E-02	7,97
P11	50	4,6	4,2	0,519	9,27E-02	6,21

According to Figure 15a) there will be no movement on the rock fill protection for the 11,5 l/s flow (for type A rock fill protection), being the nearest point to curve 1, of the modified Shields diagram, the one representative of profile P1. This curve corresponds to "occasional particle movement at some locations" (see legend of Figure 1). In fact, during the tests no erosion or scour was noticed, only some rock material instability was remarked.

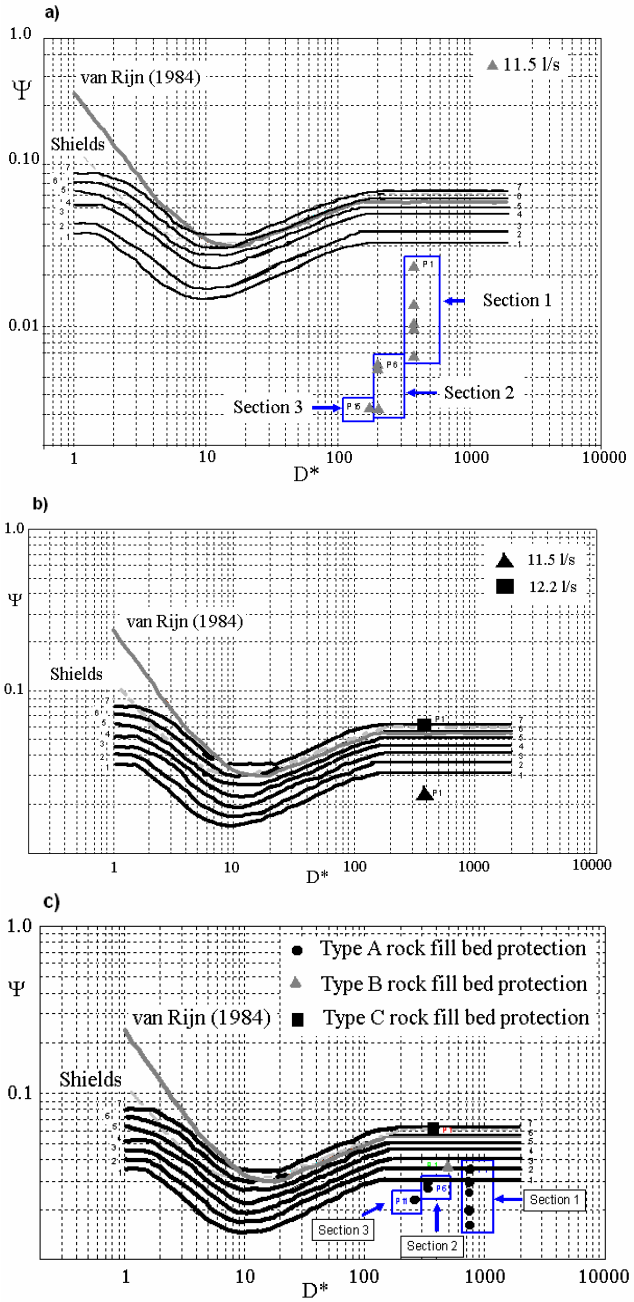

Figure 15. Modified Shields diagram for: a) 11,5 l/s flow and type A rock fill bed protection; b) 11,5 l/s and 12,2 l/s and type A rock fill protection; c) 12,2 l/s and types A, B and C rock fill protection (assuming uniform flow case).

Figure 15b) enabled comparison of Shield diagram plots correspondent to profile P1 for this

case (type A), for different flow conditions (Q= 11,5 l/s and 12,2 l/s). The point representative of the 12,2 l/s flow value was now located between curves 6 and 7 of Shields diagram, corresponding to "permanent moving of particles" and "general transport of ripples" situations, as was, in fact, confirmed during the tests.

Figure 15c) compares Shield plots correspondent to all the rock fill protection types for 12,2 l/s flow.

For type B protection, where velocity profile P1 was measured before erosion occurrence, the diagram indicated the situation of "frequent movement of particles in some locations", which was in agreement with the experimental results.

In which regards C type rock fill bed protection, Shields diagram enabled to conclude that there will be no particle movement of materials except on profile P1 location where there will be the tendency to "occasional to frequent movement of particles". In fact, it should be pointed out that, during the experiments, no erosion events of bed protection on sections 1 and 2 were recorded. However, on section 3, some scour has occurred, as it was shown in the previously referred Figure 12.

The above analysis was based on the assumption that the studied flows were uniform flows and thus the representation of their velocity profiles could be made using the logarithmic law defined by the expression (2).

Nevertheless, velocity profiles on the inner region, corresponding to the 11,5 l/s flow case have been plotted, and shown on Figure 16. For inner limit region, the value of y'/h = 0.2, often used, was considered. Those profiles enabled to conclude that the flow, was in fact not uniform.

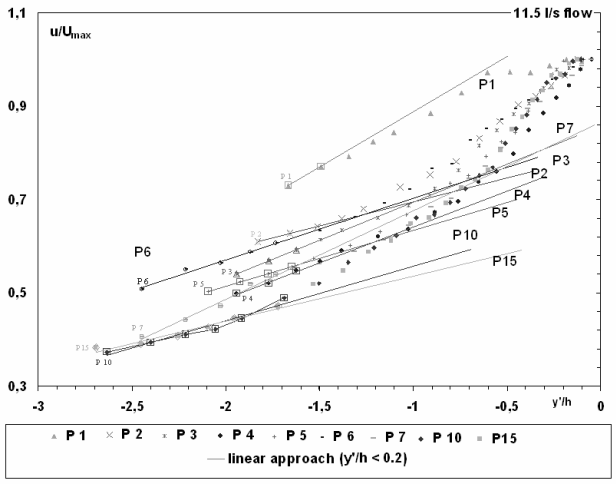

Figure 16. Uniformity flow analysis for 11,5 l/s flow.

The same conclusion could be withdrawn through Rotta criterion application, using the set of expressions (3) which values are shown on table 5 for the 12,2l/s flow and the three rock fill bed protections studied, which confirms the non-uniformity of the flow.

Table 5. Rotta criterion parameters evolution for 12,2 l/s flow and for type A, B and C rock fill bed protections: a) u_{*}/U_{max}; b) β; c) $U_{max}\delta^{*}/u_{*}$.

Profile	Rock fill bed protection								
	Type A			Type B			Type C		
	a)	b)	c)	a)	b)	c)	a)	b)	c)
P1	0,102	0,6	9,8	0,103	0,7	7,0	0,118	0,4	5,3
P2	-	-	-	-	-	-	0,121	1,4	4,8
P3	-	-	-	-	-	-	0,123	1,8	4,6
P4	-	-	-	-	-	-	0,119	1,2	5,8
P5	-	-	-	-	-	-	0,116	1,6	7,0
P6	-	-	-	-	-	-	0,101	2,2	8,3
P7	-	-	-	-	-	-	0,103	2,1	7,4
P8	-	-	-	-	-	-	0,105	1,6	6,9
P11	-	-	-	-	-	-	0,089	0,7	13,3

Based on the data obtained from the velocity profiles measured and for the different test conditions, velocity friction values have then been recalculated using equation (6). Table 6 presents an example of those calculations for the same case as in table 4: 12,2 l/s flow and type C rock fill protection.

Table 6. Friction velocity values evaluation for 12,2 l/s flow value and type C rock fill protection (non-uniform flow)

Profile	x	h	u^2_{*}	u_{*}
	cm	cm	cm^2/s^2	cm/s
P1	0	2,4	173,36	13,17
P2	5	2,6	78,32	8,85
P3	10	3,0	164,60	12,83
P4	15	3,4	66,87	8,18
P5	20	3,6	18,10	4,25
P6	25	3,8	27,37	5,23
P7	30	4,0	19,99	4,47
P8	35	4,2	12,91	3,59
P11	50	4,6	192,73	13,88

The same procedure has been applied to all the flow values and bed fill protection types and have been on the basis of Shields parameters recalculation for all set of flows and rock fill bed protections, which are shown on Figure 17.

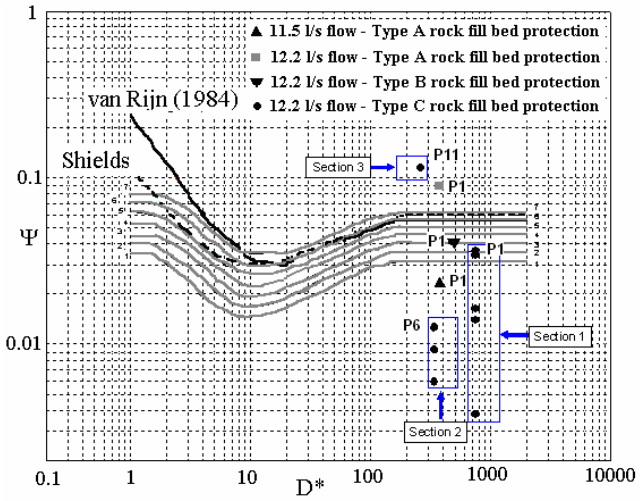

Figure 17. Modified Shields diagram for 11,5 l/s and 12,2 l/s flows and for type A, B and C rock fill bed protections, assuming the non uniform flow case.

The plotted values considering the non-uniformity conditions show to be in better agreement with the experiments. From the above figure, it can be concluded that for A and B rock type protections movement of materials shall occur, which was confirmed by the experiments, and that for C type only on section 3 of the rock fill protection, profile P11, erosion will occur, in accordance with what was, in fact, reported on experiments and shown on Figure 12. That occurrence could not be confirmed by Shields diagram when considering uniform flow case.

6. CONCLUSIONS

A physical model of Crestuma dam was made and tested for two flow values and for three different types of rock fill bed protections, in order to have a better insight on flow energy dissipation effect on those protections.

Laser Doppler anemometry was used for flow velocity measurements in order to define the corresponding flow fields on the different test conditions. Velocity profiles measurements at different locations in the stilling basin and in the downstream rock fill bed protection, allowed the definition of the mean and turbulent flow field characteristics corresponding to each one of the different test conditions.

Two different limit flow discharges were studied, enabling the analysis of scour effects on different rock fill bed protections; one close to incipient motion of particles of (type A) rock fill bed protection and the other with scouring effects on the three different studied (growing in dimension, types A, B and C) rock fill types.

Critical shear stress criterion, using modified Shields diagram was applied to analyse the different types of rock fill bed protection behaviour. Subsequently, Shields parameters have been calculated assuming uniformity or non-uniformity behaviour of the flow.

Based on the above criterion scour occurrence was analysed and experimental results compared with the theoretical ones.

It could be concluded that, in general, the non-uniform flow approach led to better results on scour occurrence analysis.

Future work shall be made taking into account other different criteria for initiation of sediments movement in order to compare the obtained results.

ACKNOWLEGEMENTS

The authors are grateful to FCT who funded this work through the project POCTI/ECM/36031/2000 “Energy Dissipation in Hydraulic Structures Established on Mobile Bed”.

REFERENCES

Cardoso, A. H. 1990. *Spatially Accelerating Flow in a Smooth Open Channel, These N.º 813 (1989),* Ecole Polythechnique Fédérale de Lausanne.

Chang, H. H. 1988. Fluvial processes in river engineering. John Wiley & Sons.

Graf, W. H. & Song, T. 1995. Bed-shear stress in non-uniform and unsteady open-channel flows, *Journal for Hydraulic Research*, vol. 33: 699-703.

Graf, W. H. & Altinakar, M.S. 1998. *Fluvial Hydraulics – Flow and Transport Processes in Channels of Simple Geometry*. John Wiley & Sons.

LNEC. 1972. *Estudo hidráulico em modelo reduzido do aproveitamento de Crestuma, 1º Relatório, (Hydraulic Study of Crestuma dam in physical model, 1st Report), Laboratório Nacional de Engenharia Civil, Lisboa.*

Hoffmans, G.J.C.M. & Verheij, H.J. 1997. *Scour Manual,* Rotterdam: Balkema.